Journal of Power Sources 430 (2019) 169–174

Contents lists available at ScienceDirect

Journal of Power Sources

journal homepage: www.elsevier.com/locate/jpowsour

Induced nanoscale roughness of current collectors enhances lithium ion battery performances

Jimmy Ching-Ming Chen [a], Jinho Yang [b], Mark Ming-Cheng Cheng [b,*]

[a] Division of Engineering Technology, Wayne State University, Detroit, MI, 48202, USA
[b] Department of Electrical and Computer Engineering, Wayne State University, Detroit, MI, 48202, USA

ARTICLE INFO

Keywords:
Lithium ion battery
Silicon anode
In-situ stress measurement
White light interferometry
Current collector

ABSTRACT

In this paper, in-situ nanomechanical measurement and ex-situ morphology study were conducted to investigate the surface roughness effects of current collectors on the performance of thin film silicon anodes. The in-situ analysis quantifies electrochemical processes and associated mechanical stress such as silicon-lithium alloy formation during charge and discharge. Upon lithiation, after SEI formation (approximately below 0.35 V), both *α-Si* films deposited on the pristine and $FeCl_3$-etched copper experience elastic deformation with a rapid rise of a compressive stress. The films begin to deform plastically after the stress reaches compressive yield strength. Upon delithiation, the *α-Si* on the pristine copper has shown to have stress dissipation at a tensile stress of 0.28 GPa. However, the tensile stress of the *α-Si* on the $FeCl_3$-etched copper continues until the stress reaches 0.4 GPa at the end of delithiation. In addition, the silicon anode was found to form small islands on roughened current collector (instead of peel-off from flat current collector), indicating the design of the current collector may play an important role in the performance of lithium ion battery.

1. Introduction

The need to increase the energy and power density of lithium ion batteries for consumer electronics and electric vehicles has led to intense interest to develop high capacity electrodes. Silicon is an attractive candidate for anodes thanks to its high specific capacity (3579 mA g^{-1}) and low cost. However, the large volume expansion (~370%) associated with silicon-lithium (Si-Li) alloy formation causes pulverization of electrode material and poor cyclic performance. Recently, engineering nanostructures and thin films have been found to be an appealing approach to overcome material degradation [1–4]. Silicon nanostructures have been shown to accommodate large volume expansion and to mitigate mechanical stress [5–8]. Nevertheless, the capacity retention of silicon-based anodes over many cycles is still problematic [9]. Two of the main challenges are the loss of electrical contact between active materials and delamination of material from the substrate (current collector).

In order to minimize electrical contact loss between the silicon active material and the current collector, several studies have been conducted to optimize the architecture of current collectors, including roughening substrates by mechanical or chemical treatments [10–15] as well as engineering three-dimensional substrates such as metal foams and porous copper [16–19]. The cyclic performance of silicon anodes with roughened substrates has been shown improved. The improvement is attributable to better adhesion between the active material and the substrate.

Lee et al. adapted cantilevers to monitor 35 nm Si anodes during charge and discharge [20], but the study did not provide any quantitative information. Sethuraman et al. studied the stress evolution of a thin film Si anode using the curvature changes of substrates and Stoney's equation [21,22]. The compressive yield strength reached −1.75 GPa and the Si film began to flow plastically. With further lithiation, the stress eventually decreased to −1 GPa. However, the measured stress was an average value over a wafer-scale substrate. In their experiment, the stress variation is developed by only the lithiated Si and the profile includes elastic and plastic responses. To the best of our knowledge, all of these measurements were not sensitive enough to distinguish critical electrochemical processes, such as solid-electrolyte interphase (SEI) and Si-Li alloy formations. SEI is a passivation layer that forms on the electrode surface during the first cycle due to the decomposition of electrolytes [23,24]. On the other hand, SEI is electrically insulating and protects stored lithium atoms from electrolytes. However, there has

* Corresponding author. 5050 Anthony Wayne Drive #3140, Detroit, MI, 48202, USA.
E-mail address: mcheng@wayne.edu (M.M.-C. Cheng).

https://doi.org/10.1016/j.jpowsour.2019.05.026
Received 1 February 2019; Received in revised form 22 April 2019; Accepted 6 May 2019
Available online 16 May 2019
0378-7753/

been no in-situ study to quantify how the roughened substrate accommodates the volume expansion of the Si-Li alloy as well as it's impacts on surface topology.

In this work, volume expansion and stress evolution according to the substrate roughness are studied by observing the electrochemical processes of silicon active materials evaluated on the pristine and roughened copper substrates during the charge and discharge cycles. The processes are characterized using bilayered cantilever beams made of silicon and copper. The mass of SEI layers and mechanical stress of Si-Li alloys cause the bending of cantilevers. This paper reported for the first time monitoring the surface profiles and microstructures of battery materials in real time using a white light interferometer and cantilevers for in-situ measurement. The combination allows not only in-situ strain measurements of battery materials during charging/discharging but also observations of cracking patterns. In addition, novel techniques have been used to measure mass change of battery materials during cycling [25].

2. Experiment background, results and discussion

A series of experiments were designed to compare silicon active material stress evolutions on charge/discharge cycles, as well as silicon adhesion and cracking sizes between samples with different roughness of copper substrates. Active material stress evolutions were measured on cantilever beams, whose fabrication process is demonstrated in Fig. S1. The roughness of copper was the experiment treatment and was measured by AFM before and after $FeCl_3$-etching (Fig. S2). The root-mean-square roughness (R_q) of pristine and etched copper samples was 17 nm and 182 nm, respectively. The roughness of the samples after amorphous silicon (*a*-Si) deposition became 16 nm and 187 nm, respectively, suggesting that *α-Si* was uniformly evaporated. Scotch tape was used to test the adhesion of these bilayer samples. The *α-Si* deposited on etched copper had better adhesion than that on pristine copper (Fig. S3). Most material characterization of the deposited *α-Si has been published in other paper*, including CV, EIS, XPS and TEM [6].

2.1. Stress evolution

Fig. 1a demonstrated the picture of the in-situ cantilever beam stress measurement system. A white light interferometer was adapted to measure the curvature of a cantilever sample by monitoring its three-dimensional profiles. The fidelity of the measurement is comparable with the optical-lever detection used in Lee's work, which is a detection of a single-point deflection [20]. A potentiostat is used to charge/discharge the sample and monitor its voltage changes during cycles. The sample is composed of several bilayer cantilever beams with a silicon thin film deposited on a copper substrate sealed in a testing cell filled with electrolyte, as shown in Fig. 1b. The Young's modulus and yield strength of copper were reported to be 117 GPa and 116 MPa, respectively [26]. The yield strength sets the ceiling of the applied stress for reversible deformation of the material. The length and thickness of the cantilevers are 1 mm and 25 μm, respectively, while the width varies from 0.1 to 0.3 mm.

The surface lithium ion absorption and/or the volume expansion of the *α-Si* thin film cause the free-standing cantilever to bend. The film stress on a bilayer cantilever has been studied analytically and reported by Timoshenko [27] as,

$$\sigma_f = \frac{k \cdot E_{Si} \cdot h_t [3(1+m)^2 + (1+mn)(m^2 + \frac{1}{mn})]}{6(1+m)^2} \quad (1)$$

where σ_f is the film stress, k is the curvature change of a cantilever, n is the ratio of the thickness of silicon to copper ($n = h_{si}/h_{cu}$), h_t is the total thickness ($h_t = h_{si} + h_{cu}$), and m is the ratio of Young's moduli of silicon to copper ($m = E_{si}/E_{cu}$). The equation is under the assumptions including (1) the deformation of copper is within an elastic range. (The cantilever curvature k at full lithiation was in the range of 1/30 to 1/20 mm^{-1}. Taking the upper limit, the maximum strain of the copper substrate is approximately $\varepsilon = k\ h_{cu}/2 = 0.625$ μ, the corresponding stress is $\sigma = \varepsilon E_{cu} = 68.8$ kPa, which is much smaller than the copper tensile yield strength. Therefore, the deformation of copper is expected to be within the elastic range.), and (2) the width of a cantilever is small compared to its length [28] (The length of the cantilevers is 1 mm, and the width varies from 0.1 to 0.3 mm. The maximum ratio is 0.3, which can be regarded small.). The thickness of the active material depends on the charging state and is expressed as $h_{si} = h_{si}^0(1+\beta z)$, where z is the state of charge ($0 < z < 1$), and h_{si}^0 is the initial thickness of Si. β is assumed to be 2.7 when the maximum volume expansion is 370% for fully lithiated silicon ($Li_{3.75}Si$), equivalent to a specific capacity of 3579 $mAhg^{-1}$ [29,30]. In this work, β was calculated using Coulomb counting. Because of the constraint from the substrate, only the height of the *α-Si* was assumed to change upon lithiation and delithiation while the length and width remain fixed. The Young's modulus of the *α-Si* film also varied depending on the state of charge. The Si-Li alloy became softer than the pure *α-Si* (90 GPa). Using density function theory [31], the elastic modulus of the fully lithiated $Li_{3.75}Si$ has been calculated to be 34 GPa.

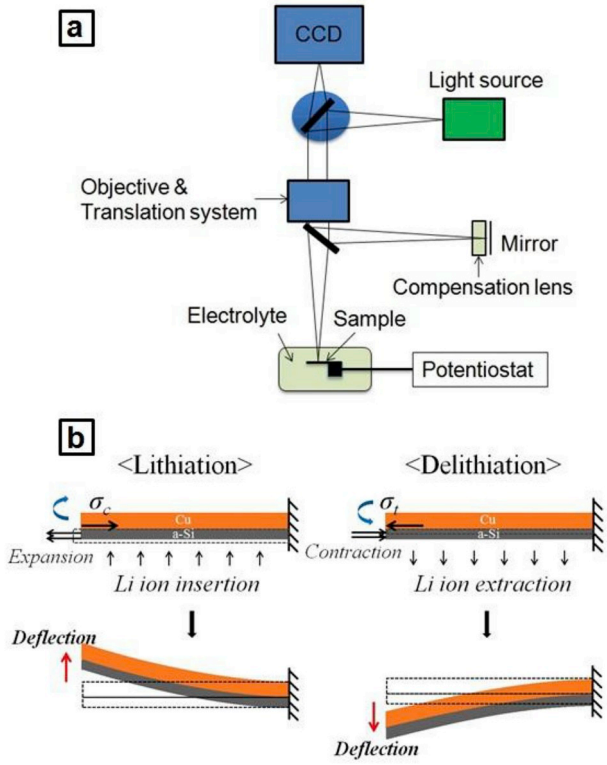

Fig. 1. (a) Optical setup and (b) working principle of the in-situ measurement.

Fig. 2 shows the first-cycle charge and discharge curves of the samples with 250 nm *α-Si* films deposited on the pristine and etched copper substrates, and their corresponding stress profiles. The black curve demonstrates the results of *α-Si* on pristine copper. During the initial lithiation, the voltage dropped accordingly until a voltage plateau appeared below 0.35 V. The stress was negligible while the voltage was above 0.35 V, but increased dramatically below 0.35 V. The stress profiles indicate a distinct electrochemical process, known as SEI formation on electrodes mostly in the beginning of the first cycle [23,24]. In this experimental setup, heavy SEI formation occurred above 0.35 V and stemmed from the excessive consumption of electrolytes due to the suspended cantilevers in the liquid chamber.

Below 0.35 V, compressive stress increased rapidly due to volume expansion caused by the insertion of lithium in silicon. At the beginning of the Si-Li alloy formation, the stress began increasing linearly over

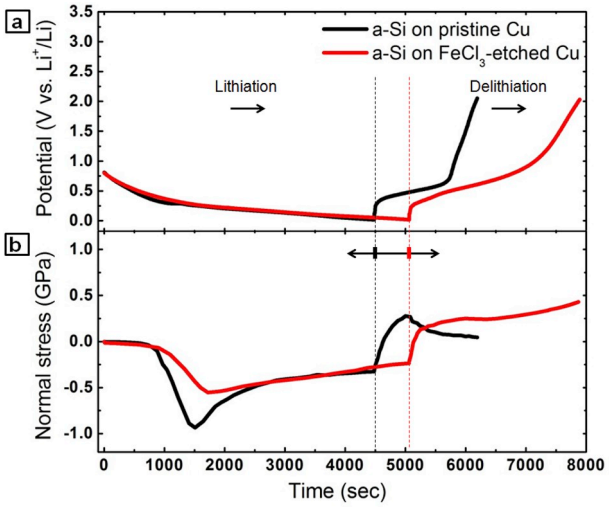

Fig. 2. (a) Voltage and (b) in-situ stress profiles of the *a*-Si films on the pristine (black) and $FeCl_3$-etched copper (red) cantilevers in the liquid cell chamber. (For interpretation of the references to colour in this figure legend, the reader is referred to the Web version of this article.)

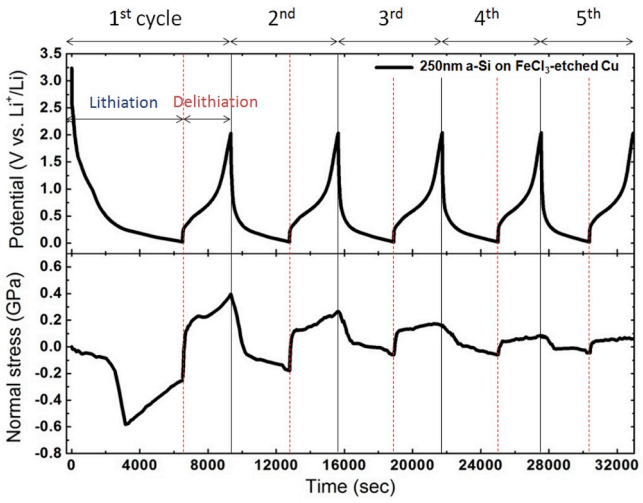

Fig. 3. Voltage (top) and in-situ stress profiles (bottom) of the *a*-Si film on the $FeCl_3$-etched copper during 5 cycles.

time, where the strain was proportional to lithium concentration in Si. For *α-Si* on the pristine copper (black line), the compressive stress reached a maximum value of −0.94 GPa. This agrees with the results of other groups, where the yield strength of lithiated silicon was reported ca. −1 GPa [32,33]. With further lithiation, silicon began to flow plastically to accommodate additional volume changes, and the stress eventually dropped to −0.33 GPa. Upon delithiation, the removal of lithium caused the volume to decrease, generating tensile stress. Initially, the tensile stress increased rapidly until it reached a maximum value of 0.28 GPa, and then dropped with further delithiation due to Si fracture [33] because the stress was relieved after crack formation. In addition, the negligible stress above 0.7 V suggests that most Si films lost their electrical contact with the copper substrates. In a similar experiment, where the cantilever was flipped over to let Si face the glass, the stress dissipation was observed at a similar voltage (Fig. S4).

The stress profile (red line) for *α-Si* on roughened copper was close to that on pristine copper. until the voltage dropping to 0.35 V during lithiation. When Si started to react with Li below 0.35 V, the compressive stress increased linearly but the slope was smaller than that of the pristine sample. The stress was reduced because the rough surfaces allowed the transverse coupling between in-plane and out-of-plane strains of silicon volume expansion [34,35]. The stress reached a maximum value of −0.58 GPa, and gradually returned to −0.25 GPa during the plastic deformation. Upon delithiation, the tensile stress of the *α-Si* on the roughened copper initially increased, and began to flow plastically when the voltage was above 0.46 V. The stress eventually reached a maximum value of 0.4 GPa at the end of delithiation. The stress measurement suggests that *α-Si* films were in good electrical contact with the roughened substrate. On the contrary, *α-Si* on pristine copper lost its electrical contact after the first cycle and no capacity remained. The delithiation time of the roughened copper sample was approximately three times longer than that of the pristine sample.

Fig. 3 shows the cell voltage and stress evolution of the roughened copper sample during the first five cycles. Upon the 2nd lithiation, compressive stress increased immediately, which indicates Si-Li alloy formation. This implies that most SEI was formed during the first cycle. The stress increased linearly to −0.1 GPa, and slightly further increased to −0.13 GPa during plastic deformation. The compressive stress was much smaller than that of the first lithiation. In addition, the stress was not reduced during the further lithiations. Combined with SEM images, the study suggests that the major cracking occurred during the first lithiation relieved the stress. The *α-Si* films adhered to the substrate after cracking and formed small Si islands. The magnitudes of stress of other cycles were much smaller than that of the first cycle, which can be attributed to the more and smaller disconnected-islands. Interestingly, the stress increased suddenly to reach a maximum value of −0.2 GPa when the voltage was below 50 mV. The sudden increase in stress was probably due to a phase transition of Si-Li alloy to a new crystalline phase, which has been demonstrated by XRD studies [4,5,23]. The stress evolution in the first five cycles followed the dynamic electrochemical processes over time. The stress was gradually relaxed over five cycles due to material degradation, and changes of morphology and chemical properties.

2.2. Cracking profiles

Fig. 4 shows the SEM images of *α-Si* films on the pristine and roughened copper after cycling. The *α-Si* on the pristine copper had large disconnected islands after the first cycle (Fig. 4a). Some islands were peeled off during the cell disassembly. In comparison, Si on the roughened copper after 5 cycles (Fig. 4b) also had separated islands but they were smaller sized and still attached to the roughened copper substrate. A critical cracking size for a Si thin film electrode was estimated as [36,37],

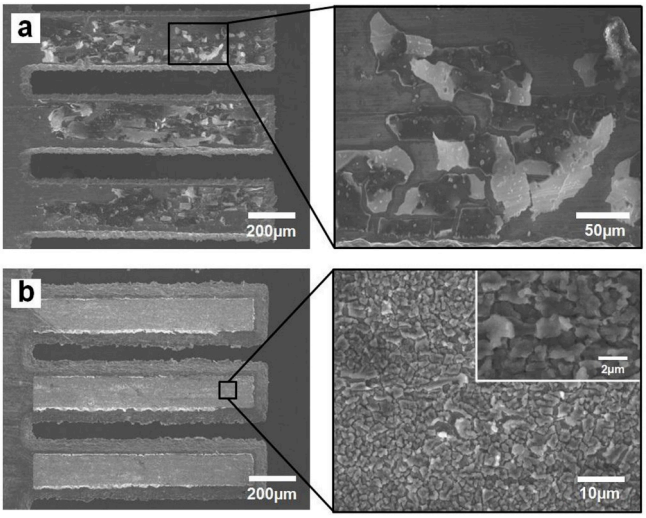

Fig. 4. SEM images of (a) the *a*-Si film on the pristine copper cantilever after 1 cycle and (b) the film on the $FeCl_3$-etched copper cantilevers after 5 cycles.

$$L_{cr} = \frac{2\sigma_Y^{Si}}{\tau_{cr}^{int}} h \quad (2)$$

where h is the thickness of Si film, and σ_Y^{Si} (0.6–0.94 GPa) is the yield strength of Si, which represents the maximum compressive stress (onset of the stress plateau). τ_{cr}^{int} is the interfacial shear strength between the lithiated Si and the substrate. The interfacial shear strength is often used to characterize the quality of adhesion between the material and substrate [38], because the shear strength varies with bonding of the interface. τ_{cr}^{int} can be estimated using both the shear flow stress of Cu (40 MPa [39]) and the interfacial friction strength τ_{fr}^{int} of the silicate composite (40.5 MPa [40]). If the actual surface profile can be described by a Fourier series as $z = \sum R_{qk} \sin\omega_k x$, where ω_k is the roughness repeating frequency and R_{qk} is the rms roughness [2]. For simplicity, consider only one mode in the z direction. We also consider the shear tensile strengths of *α-Si* (τ_{si}) or copper and assume they are close (estimated around 120 MPa [3]). Then τ_{cr}^{int} can be modified by $\tau_{cr}^{int}(x) = \tau_{si}|\sin\theta| + \tau_{fr}^{int}|\cos\theta|$, where $\tan\theta = R_q\omega\cos\omega x$. The mean value of τ_{cr}^{int} over a roughness period can be estimated as

$$\tau_{cr}^{int} = \frac{\omega}{2\pi}\left[\tau_{si}\int \frac{R_q\omega\cos\omega x}{\sqrt{1+R_q^2\omega^2\cos^2\omega x}}dx + \tau_{fr}^{int}\int \frac{1}{\sqrt{1+R_q^2\omega^2\cos^2\omega x}}dx\right] \quad (3)$$

The estimated minimum cracking size for 250 nm thick Si film was 7.4–11.5 μm on the pristine copper sample and 4.4–6.9 μm on the roughened copper sample. Observed cracking sizes of the *α-Si* on the pristine copper sample were approximately 30–40 μm (Fig. 4a). The difference might be attributable to the overestimated interfacial shear strength between *α-Si* and the pristine copper due to poor adhesion. On the other hand, observed cracking sizes of 250 nm *α-Si* on the roughened Cu were 6–7 μm after the first lithiation, which is close to the estimated value. This study suggests that the surface roughness of the current collector provides a major role on the mechanical properties.

The energy release rate is the energy dissipated per unit of newly created fracture surface area and is independent of the applied loads and material geometry. Assuming interfacial sliding formed at the interface between the thin films and substrates, the energy release rate has been derived by Hu et al. [41],

$$G = \left[\frac{\sigma}{3\tau_{cr}^{int}} + F\left(\sum\right)\right]\frac{\sigma^2 h_f}{E_f} \quad (4)$$

where σ, h_f, and E_f are the normal stress (compression or tension), thickness and Young's modulus of the silicon film, respectively. $F(\Sigma)$ is a function of Dundurs parameters, and τ_{cr}^{int} is the interfacial shear strength between silicon and copper. Dundurs parameters are defined by elasticity constants and Poisson ratio, representing the elastic mismatch between the film and the substrate [42]. On the pristine copper, the silicon volume expansion tends to produce a sliding failure along a plane that is parallel to the direction of the stress.

The fracture was observed at the peak tensile stress in this work (Fig. S4b). Thus, the tensile stress value was chosen at the onset of the stress plateau. Using $\tau_{cr}^{int} = 40$ MPa and $F(\Sigma) = 1.5$ [33,43], the fracture energy of the *α-Si* on the pristine copper was estimated to be 4.9 J m^{-2}. The interfacial shear strength can be enhanced by roughening the copper. The fracture energy of α-Si on the roughened copper was estimated as $G = 3.8$ J m^{-2} by the same Dundurs parameter $F(\Sigma) = 1.5$.

The samples were tested in coin cells. Fig. S5 shows the charge and discharge curves of evaporated *α-Si* films deposited on the (a) pristine and (b) $FeCl_3$-etched copper, and Fig. S5 (c) demonstrates their cycling performances. The samples were cycled at 1C, which is referred to 1-h charging/discharging. In this study, cathodic lithiation in the anode was referred to charge. After the initial 15 cycles, the discharge capacity of the *α-Si* on the pristine copper sample became negligible owing to the loss of electrical contact. In contrast, the *α-Si* on the $FeCl_3$-etched copper sample showed stable cyclability over 50 cycles, with a capacity retention of 81%. Fig. 5 summarizes the mechanical behaviors of *α-Si* films on the pristine and roughened copper. Interestingly, the stress value of *α-Si* on the pristine copper dropped faster than that on the roughened copper. The compressive stress caused delamination and buckling of the *α-Si* films on the pristine copper. Wrinkling of *α-Si* on pristine copper was found in the SEM picture (Fig. 5b). On the other hand, the *α-Si* adhered well to the roughened copper. Small *α-Si* islands (diameter 6–7 μm) were observed as shown in Fig. 5c. Those silicon islands had good electrical contact with copper, resulting in lithiation time longer than that of the pristine sample.

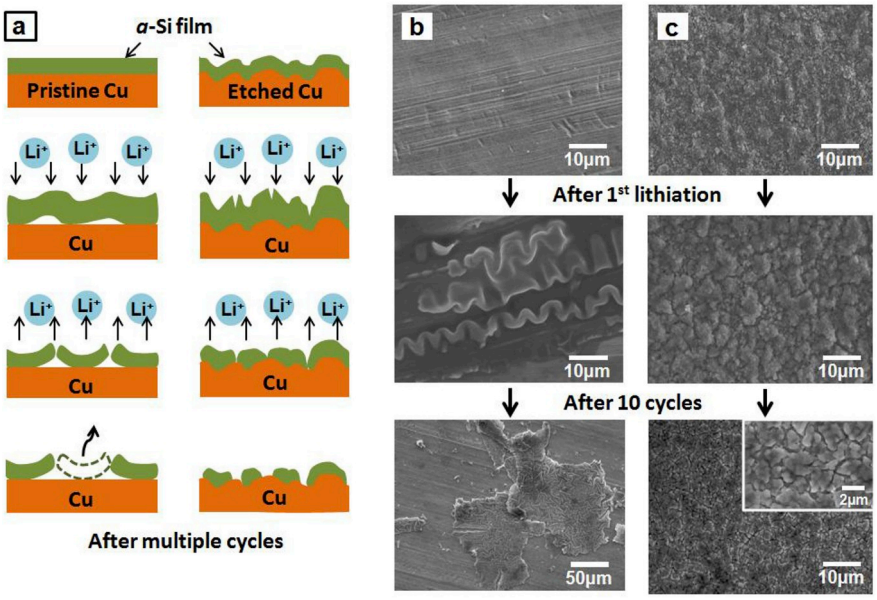

Fig. 5. (a) A schematic diagram of degradation processes of the *a*-Si anodes. The SEM images of 250 nm evaporated *a*-Si films (b) on the pristine copper and (c) $FeCl_3$-etched copper before cycling, after 1st lithiation, and after 10 cycles.

3. Conclusions

We demonstrated an in-situ mechanical analysis on the surface effect of the current collectors for lithium ion battery anodes. The analysis of surface effect was compared between Si films grown on pristine and $FeCl_3$-etched copper. The pristine copper sample showed lower Coulombic efficiency due to lost contact of active material from cracks caused by large volume changes. On the other hand, the roughened surface of the $FeCl_3$-etched sample enhanced the adhesion at the interface between the film and the copper current collector, which maintained structural stability against the volumetric increase of *α-Si* even cracks occurred. The capacity fading of the *α-Si* on the pristine copper was attributable to poor adhesion and the severe fracture of the film caused by a promoted tensile stress (0.28 GPa) during the delithiation process, where the stress dissipated. However, the tensile stress of the *α-Si* on $FeCl_3$-etched copper was retained and further promoted to 0.4 GPa, which suggests that the film was still intact with the substrate. The stress measurements allowed quantifying the fracture energy of lithiated *a*-Si. The fracture energies of $Li_{3.0}Si$ on the pristine and roughened copper were estimated to be 4.9 J m^{-2} and 3.8 J m^{-2}, respectively, at the peak tensile stress where the film began to flow plastically. This study concludes that the surface treatment of the current collector is a crucial factor in the cycling performance of the battery material.

4. Methods

Sample preparation. 25 μm thick copper foil was purchased from Lyon Industries Inc. The copper foil was first chemically etched by 0.1 M ferric chloride ($FeCl_3$) for 5 min. After etching, the copper foil was rinsed with DI water and isopropyl alcohol (IPA). The sample was dried on a heater at 70 °C for 5 min. The surface roughness before and after the chemical etching was characterized by an atomic force microscope (AFM, Veeco Dimension 3100). The average roughness was measured in a tapping mode and defined by the root mean square value from the profile. A 250 nm thick amorphous silicon (*a*-Si) was thermally evaporated by E-beam evaporation (Temescal BJD 1800) with a deposition rate of 2 Å s^{-1}.

Electrochemical test in a coin cell. The electrochemical characteristics of the *α-Si* were measured by a half-cell configuration. Cell assembly and electrochemical testing were performed in a glove box filled with ambient Argon. The cell was assembled using a CR2032 coin cell. Lithium metal (Alfa Aesar) was used as counter and reference electrodes. A polyethylene separator (Celgard 2320) was soaked overnight in the liquid electrolyte (1 mol $LiPF_6$ in ethylene carbonate (EC) and dimethyl carbonate (DMC) with a 1:1 ratio). The charge and discharge tests were performed using a potentiostat (Maccor Model 4200) at a constant current density of 2 A/g and the cut-off voltages were set at 0.02 V and 2 V versus Li^+/Li.

Characterization. After electrochemical tests, cells were disassembled and then rinsed with DMC solvent. SEM (JEOL JSM-6510LV) was used to image surface morphologies of samples before and after cycling. The acceleration voltage was 15 kV in SEM.

Preparation of cantilevers. Two kinds of copper foil (25 μm thick) were prepared: one was pristine, and the other was chemically etched ($FeCl_3$). In Fig. S1 (a) A 250 nm thick *α-Si* was deposited on as-prepared copper foil using E-beam evaporation at room temperature. (b) The *α-Si* coated copper foil was glued to a silicon wafer using a photoresist (AZ4620, Hoechst). (c,d) A photoresist (S1811, Shipley) was spin-coated and patterned by photolithography. (e) *α-Si* layer was etched by reactive ion etching (SF_6). (f,g) Second photolithography was performed. (h) The copper foil was selectively etched by a copper etchant (APS100, Transene). The cantilever was released by removing photoresist in Acetone.

In-situ characterization in a liquid cell. A free-standing cantilever composed of copper (Cu) and active material (*a*-Si) was placed in a home-made liquid cell. The cantilever faced lithium metal covered by a separator (Celgard 2320) with a space filled with electrolyte. The presence of the separator and a Teflon spacer prevents a short circuit between the anode and lithium metal. Copper serves as both a current collector and a mechanical support. During the lithiation (charging), Li ions are driven from lithium metal to anode through the electrolyte by the electrochemical potential differences between the two counter electrodes. A white light interferometry (ContourGT In-motion, Bruker) was used to measure the curvature of the cantilever during electrochemical cycling controlled by a potentiostat (Gamry G300).

Acknowledgements

The authors would like to thank Dan Durisin and Bill Funk for their assistances using nFab facility. The financial supports from National Science Foundation, USA (NSF1711409, NSF1849578), WSU and Richard Barber Foundation are gratefully acknowledged.

Appendix A. Supplementary data

Supplementary data to this article can be found online at https://doi.org/10.1016/j.jpowsour.2019.05.026.

References

[1] U. Kasavajjula, C.S. Wang, A.J. Appleby, Nano- and bulk-silicon-based insertion anodes for lithium-ion secondary cells, J. Power Sources 163 (Jan 1 2007) 1003–1039.
[2] J.R. Szczech, S. Jin, Nanostructured silicon for high capacity lithium battery anodes, Energy Environ. Sci. 4 (2011) 56–72.
[3] A.S. Arico, P. Bruce, B. Scrosati, J.M. Tarascon, W. Van Schalkwijk, Nanostructured materials for advanced energy conversion and storage devices, Nat. Mater. 4 (May 2005) 366–377.
[4] S.D. Beattie, D. Larcher, M. Morcrette, B. Simon, J.M. Tarascon, Si electrodes for li-ion batteries - a new way to look at an old problem, J. Electrochem. Soc. 155 (2008) A158–A163.
[5] J. Graetz, C.C. Ahn, R. Yazami, B. Fultz, Highly reversible lithium storage in nanostructured silicon, Electrochem. Solid State Lett. 6 (Sep 2003) A194–A197.
[6] R. Teki, M.K. Datta, R. Krishnan, T.C. Parker, T.M. Lu, P.N. Kumta, et al., Nanostructured silicon anodes for lithium ion rechargeable batteries, Small 5 (2009) 2236–2242.
[7] W. Wang, P.N. Kumta, Nanostructured hybrid silicon/carbon nanotube heterostructures: reversible high-capacity lithium-ion anodes, ACS Nano 4 (2010) 2233–2241.
[8] C.K. Chan, H. Peng, G. Liu, K. McIlwrath, X.F. Zhang, R.A. Huggins, et al., High-performance lithium battery anodes using silicon nanowires, Nat. Nanotechnol. 3 (Jan 2008) 31–35.
[9] W.J. Zhang, A review of the electrochemical performance of alloy anodes for lithium-ion batteries, J. Power Sources 196 (Jan 1 2011) 13–24.
[10] T. Takamura, S. Ohara, M. Uehara, J. Suzuki, K. Sekine, A vacuum deposited Si film having a Li extraction capacity over 2000 mAh/g with a long cycle life, J. Power Sources 129 (Apr 15 2004) 96–100.
[11] Y.L. Kim, Y.K. Sun, S.M. Lee, Enhanced electrochemical performance of silicon-based anode material by using current collector with modified surface morphology, Electrochim. Acta 53 (May 20 2008) 4500–4504.
[12] J.T. Yin, M. Wada, K. Yamamoto, Y. Kitano, S. Tanase, T. Sakai, Micrometer-scale amorphous Si thin-film electrodes fabricated by electron-beam deposition for Li-ion batteries, J. Electrochem. Soc. 153 (2006) A472–A477.
[13] C.M. Hwang, C.H. Lim, J.H. Yang, J.W. Park, Electrochemical properties of negative SiMox electrodes deposited on a roughened substrate for rechargeable lithium batteries, J. Power Sources 194 (Dec 1 2009) 1061–1067.
[14] D. Reyter, S. Rousselot, D. Mazouzi, M. Gauthier, P. Moreau, B. Lestriez, et al., An electrochemically roughened Cu current collector for Si-based electrode in Li-ion batteries, J. Power Sources 239 (Oct 1 2013) 308–314.
[15] C.C. Nguyen, S.W. Song, Interfacial structural stabilization on amorphous silicon anode for improved cycling performance in lithium-ion batteries, Electrochim. Acta 55 (Mar 1 2010) 3026–3033.
[16] G.F. Yang, J.S. Song, H.Y. Kim, S.K. Joo, Metal foam as positive electrode current collector for LiFePO4-based Li-ion battery, Jpn. J. Appl. Phys. 52 (Oct 2013).
[17] Q.N. Sa, Y. Wang, Ni foam as the current collector for high capacity C-Si composite electrode, J. Power Sources 208 (Jun 15 2012) 46–51.
[18] X.Y. Fan, F.S. Ke, G.Z. Wei, L. Huang, S.G. Sun, Sn-Co alloy anode using porous Cu as current collector for lithium ion battery, J. Alloy. Comp. 476 (May 12 2009) 70–73.
[19] W. Xu, N.L. Canfield, D.Y. Wang, J. Xiao, Z.M. Nie, X.A.H.S. Li, et al., An approach to make macroporous metal sheets as current collectors for lithium-ion batteries, J. Electrochem. Soc. 157 (2010) A765–A769.

[20] S.J. Lee, J.K. Lee, S.H. Chung, H.Y. Lee, S.M. Lee, H.K. Baik, Stress effect on cycle properties of the silicon thin-film anode, J. Power Sources 97–8 (Jul 2001) 191–193.
[21] V.A. Sethuraman, M.J. Chon, M. Shimshak, V. Srinivasan, P.R. Guduru, In situ measurements of stress evolution in silicon thin films during electrochemical lithiation and delithiation, J. Power Sources 195 (Aug 1 2010) 5062–5066.
[22] M.J. Chon, V.A. Sethuraman, A. McCormick, V. Srinivasan, P.R. Guduru, Real-time measurement of stress and damage evolution during initial lithiation of crystalline silicon, Phys. Rev. Lett. 107 (Jul 21 2011).
[23] T.D. Hatchard, J.R. Dahn, In situ XRD and electrochemical study of the reaction of lithium with amorphous silicon, J. Electrochem. Soc. 151 (2004) A838–A842.
[24] M. Winter, J.O. Besenhard, M.E. Spahr, P. Novak, Insertion electrode materials for rechargeable lithium batteries, Adv. Mater. 10 (Jul 9 1998) 725–763.
[25] J.H. Yang, J. Chen, M.M.C. Cheng, In-situ monitor electrochemical processes in batteries using vibrating microcantilevers, in: 2014 Ieee International Frequency Control Symposium, Ieee, New York, 2014, pp. 28–31.
[26] D.Y.W. Yu, F. Spaepen, The yield strength of thin copper films on Kapton, J. Appl. Phys. 95 (Mar 15 2004) 2991–2997.
[27] W.L. Fang, H.C. Tsai, C.Y. Lo, Determining thermal expansion coefficients of thin films using micromachined cantilevers, Sensor Actuator Phys. 77 (Sep 28 1999) 21–27.
[28] S. Timoshenko, Analysis of bi-metal thermostats, J. Opt. Soc. Am. Rev. Sci. Instrum. 11 (Sep 1925) 233–255.
[29] M.N. Obrovac, L. Christensen, Structural changes in silicon anodes during lithium insertion/extraction, Electrochem. Solid State Lett. 7 (2004) A93–A96.
[30] M.N. Obrovac, L.J. Krause, Reversible cycling of crystalline silicon powder, J. Electrochem. Soc. 154 (2007) A103–A108.
[31] V.B. Shenoy, P. Johari, Y. Qi, Elastic softening of amorphous and crystalline Li-Si Phases with increasing Li concentration: a first-principles study, J. Power Sources 195 (Oct 1 2010) 6825–6830.
[32] S.P.V. Nadimpalli, V.A. Sethuraman, G. Bucci, V. Srinivasan, A.F. Bower, P. R. Guduru, On plastic deformation and fracture in Si films during electrochemical lithiation/delithiation cycling, J. Electrochem. Soc. 160 (2013) A1885–A1893.
[33] M. Pharr, Z.G. Suo, J.J. Vlassak, Measurements of the fracture energy of lithiated silicon electrodes of Li-ion batteries, Nano Lett. 13 (Nov 2013) 5570–5577.
[34] A. Li, V. Ji, J.L. Lebrun, G. Ingelbert, Surface-roughness effects on stress determination by the X-ray-diffraction method, Exp. Tech. 19 (Mar-Apr 1995) 9–11.
[35] O. Ergincan, G. Palasantzas, B.J. Kooi, Influence of random roughness on cantilever curvature sensitivity, Appl. Phys. Lett. 96 (May 31 2010) (vol 96, 041912, 2010.
[36] X. Xiao, P. Liu, M.W. Verbrugge, H. Haftbaradaran, H. Gao, Improved cycling stability of silicon thin film electrodes through patterning for high energy density lithium batteries, J. Power Sources 196 (Feb 1 2011) 1409–1416.
[37] S.K. Soni, B.W. Sheldon, X. Xiao, M.W. Verbrugge, D. Ahn, H. Haftbaradaran, et al., Stress mitigation during the lithiation of patterned amorphous Si islands, J. Electrochem. Soc. 159 (2012) A38–A43.
[38] R.W. Carpick, N. Agrait, D.F. Ogletree, M. Salmeron, Variation of the interfacial shear strength and adhesion of a nanometer-sized contact, Langmuir 12 (Jun 26 1996) 3334–3340.
[39] K.J. Frutschy, R.J. Clifton, High-temperature pressure-shear plate impact experiments on OFHC copper, J. Mech. Phys. Solids 46 (Oct 1998) 1723–1743.
[40] Q.Y. Li, K.S. Kim, Micromechanics of friction: effects of nanometre-scale roughness, Proc. Math. Phys. Eng. Sci. 464 (May 8 2008) 1319–1343.
[41] M.S. Hu, A.G. Evans, The cracking and decohesion of thin-films on ductile substrates, Acta Metall. 37 (Mar 1989) 917–925.
[42] J.C.W. Vanvroonhoven, Analysis of stress singularities in Bi-material interfaces with applications to ic packaging, in: Ecf 9 - Reliability and Structural Integrity of Advanced Materials vol. I, 1992, pp. 1315–1320 and Ii.
[43] J.L. Beuth, Cracking of thin bonded films in residual tension, Int. J. Solids Struct. 29 (1992) 1657–1675.